DALTON
FULL PAPER

Co-ordination chemistry of 6-(2-hydroxyphenyl)pyridine-2-carboxylic acid: a terdentate ligand with a mixed phenolate/pyridyl/carboxylate donor set †

Samantha M. Couchman,[a] John C. Jeffery,[a] Peter Thornton[b] and Michael D. Ward *,[a]

[a] *School of Chemistry, University of Bristol, Cantock's Close, Bristol, UK BS8 1TS*
[b] *Department of Chemistry, Queen Mary and Westfield College, Mile End Road, London, UK E1 4NS*

The new ligand 6-(2-hydroxyphenyl)pyridine-2-carboxylic acid (H_2L) having a terdentate phenolate–pyridyl–carboxylate (O,N,O) donor set has been found to co-ordinate to transition-metal and lanthanide(III) ions as a dianionic terdentate chelate. The complexes $K[M^{III}L_2]$ (M = Cr or Fe) are both octahedral with a *trans*-N_4O_2 donor set, and according to X-ray analysis have the K^+ ion associated with the complex anion *via* interactions with phenolate and carboxylate oxygen atoms of the ligands. The iron(III) complex is high spin according to EPR and UV/VIS spectroscopy, and is structurally similar to iron(III) complexes of natural siderophores such as desferriferrithiocin. Two dinuclear copper(II) complexes were crystallographically characterised: $[Cu_2L_2(MeOH)_2]$ has a planar $\{Cu_2L_2\}$ core with two phenolate ligands bridging the copper(II) centres, and an axial MeOH ligand on each Cu atom, one directed to either side of the $\{Cu_2L_2\}$ core; in $[Cu_2L_2(MeOH)(H_2O)]$ in contrast the axial solvent molecules, one H_2O and one MeOH, are both on the same face of the $\{Cu_2L_2\}$ core which induces a substantial 'bowing' of the core to minimise steric interference between them. The terbium(III) complex $K[TbL_2(H_2O)_2]\cdot 2H_2O$ was also prepared, and has eight-co-ordination; there is an extensive hydrogen-bonding network involving the K^+ ions and water molecules. Luminescence spectroscopic studies in MeOH and MeOD gave a value of 4.9 for the number of co-ordinated solvent molecules (q), consistent with an additional contribution to quenching from hydrogen-bonded solvent molecules, and/or partial dissociation of the L^{2-} moieties.

As part of our continuing programme of research into the co-ordination chemistry of new polydentate ligands,[1] we describe in this paper the synthesis and co-ordination behaviour of the mixed-donor terdentate chelating ligand 6-(2-hydroxyphenyl)-pyridine-2-carboxylic acid (H_2L), which contains phenolate, pyridyl and carboxylate donor atoms. We were interested in this donor set for two reasons. First, it is relevant to the biological chemistry of metal ions in the +3 oxidation state, particularly Fe^{III}.[2] The iron–tyrosinate metalloproteins, which include the transferrins, catechol dioxygenases and purple acid phosphatases, contain mixed donor sets comprising phenolate (from tyrosine), unsaturated nitrogen (from histidine) and carboxylate (from aspartate or glutamate).[3] Suitable ligands to prepare model complexes, in order to probe the structural and spectroscopic properties of the active sites, must therefore mimic this combination of donors.[4,5] The phenolate/imine/carboxylate donor set also closely mimics the donor set of the natural siderophore desferriferrithiocin,[6] derivatives of which have recently been investigated as therapeutic iron chelators for clinical use.[7] Secondly, the relatively hard donor set should be appropriate for co-ordination of lanthanide(III) ions. Complexes of Tb^{III} and Eu^{III} with polydentate aromatic ligands based on (*inter alia*) mixed pyridyl/carboxylate donors are of particular interest for their luminescence properties following sensitisation of the metal-centred luminescence by energy transfer from a ligand-centred excited state,[8] and we have been interested in studying the structures and properties of luminescent lanthanide complexes with multidentate chelating ligands containing aromatic chromophores.[9,10] The synthesis of H_2L is herein described, together with the syntheses, crystal structures and properties of its complexes with Cr^{III}, Fe^{III}, Cu^{II} and Tb^{III}.

† *Non-SI units employed*: G = 10^{-4} T, $\mu_B \approx 9.27 \times 10^{-24}$ J T^{-1}.

Experimental

General

Instrumentation used for routine spectroscopic, electrochemical and luminescence studies has been described previously.[9] 2-(2-Methoxyphenyl)pyridine was prepared according to the published method.[11] Reagents were obtained commercially (from Aldrich or Avocado) and used as received. Magnetic susceptibilities were measured over a range of temperatures down to 77 K using a Faraday balance calibrated with $HgCo(NCS)_4$ as described previously.[12]

Preparations

2-(2-Methoxyphenyl)pyridine *N*-oxide 1. This preparation is based on a published method.[13] To a solution of 2-(2-methoxyphenyl)pyridine (9.019 g, 0.048 mol) in glacial acetic acid (30 cm^3) was added H_2O_2 (30% solution in water, 5 cm^3). After stirring the mixture at 80 °C for 3 h an additional portion of H_2O_2 (30% solution in water, 5 cm^3) was added. After stirring overnight at 80 °C a golden-yellow solution was obtained, which was reduced in volume to *ca.* 10 cm^3. The residue was diluted with water (20 cm^3) and then treated with K_2CO_3 until a yellow precipitate appeared, which was extracted with several portions of CH_2Cl_2. The combined organic extracts were dried ($MgSO_4$) and evaporated to dryness. The solid was purified by column chromatography on silica using CH_2Cl_2 containing a small amount of MeOH (0.5% v/v) as eluent. After traces of starting material, the product was collected as the second fraction. Yield: 8.64 g (88%). EI mass spectrum: *m*/*z* 201 (M^+) and 170 (M^+ − OMe). ^{1}H NMR (300 MHz, $CDCl_3$): δ 8.33 (1 H, m, pyridyl H^6), 7.48–7.32 (3 H, m), 7.30–7.20 (2 H, m), 7.10–7.00 (2 H, m) and 3.82 (3 H, s, OMe) (Found: C, 71.5; H, 5.5; N, 7.1. $C_{12}H_{11}NO_2$ requires C, 71.6; H, 5.5; N, 7.0%).

2-Cyano-6-(2-methoxyphenyl)pyridine 2. This preparation is based on a published method.[14] To a solution of compound **1** (4.00 g, 19.9 mmol) in dry MeCN (50 cm^3) under N_2 was added dry Et_3N (3.02 g, 4.2 cm^3, 30 mmol) by syringe. The mixture was stirred with gentle warming for a few minutes, and then Me_3SiCN (5.0 g, 50 mmol) was also added *via* syringe. The mixture was heated to reflux for 18 h, and then allowed to cool. To destroy the excess of Me_3SiCN, aqueous $NaHCO_3$ was added slowly until a cream precipitate appeared which redissolved on addition of more water. The solvent was then removed *in vacuo* and the alkaline residue extracted into several portions of CH_2Cl_2, which were combined, dried ($MgSO_4$) and evaporated to dryness. Purification by column chromatography on silica using CH_2Cl_2 afforded pure **2** as the first and major fraction. Yield: 4.18 g (79%). EI mass spectrum: *m*/*z* 209 (M^+) and 179 ($M^+ - OMe$). ^1H NMR (300 MHz, $CDCl_3$): δ 8.12 (1 H, dd, *J* 8.2, 1.0, pyridyl H^3 or H^5), 7.86 (1 H, dd, *J* 7.7, 1.8, phenyl H^3 or H^6), 7.82 (1 H, t, *J* 8.2, pyridyl H^4), 7.60 (1 H, dd, *J* 7.5, 1.1, pyridyl H^5 or H^3), 7.43 (1 H, ddd, *J* 8.3, 7.5, 1.8, phenyl H^4 or H^5), 7.11 (1 H, td, *J* 7.5, 0.9, phenyl H^5 or H^4), 7.02 (1 H, dd, *J* 8.3, 0.9 Hz, phenyl H^6 or H^3) and 3.88 (3 H, s, OMe) (Found: C, 74.1; H, 4.7; N, 13.3. $C_{13}H_{10}N_2O$ requires C, 74.3; H, 4.8; N, 13.3%).

6-(2-Hydroxyphenyl)pyridine-2-carboxylic acid (H_2L). A solution of compound **2** (0.516 g, 2.5 mmol) in 47% aqueous HI (30 cm^3) was heated to reflux under N_2 in the dark for 2 d. The HI was then removed *in vacuo* and the solid residue washed with water and then CH_2Cl_2, and air-dried to give pure H_2L as a yellow powder. Yield: 0.475 g (90%). EI mass spectrum: *m*/*z* 215 (M^+) and 169 ($M^+ - HCO_2H$). ^1H NMR (300 MHz, CD_3SOCD_3): δ 14.1 (br s, phenolic OH), 8.45 (1 H, d, *J* 7.7, pyridyl H^3 or H^5), 8.20 (1 H, t, *J* 7.9, pyridyl H^4), 8.10 (1 H, dd, *J* 8.3, 1.7, phenyl H^3 or H^6), 8.04 (1 H, d, *J* 7.7 Hz, pyridyl H^5 or H^3), 7.36 (1 H, m, phenyl H^4 or H^5) and 6.96 [2 H, m, phenyl (H^6 or H^3) and (H^5 or H^4)] (Found: C, 66.7; H, 4.1; N, 6.4. $C_{12}H_9NO_3$ requires C, 67.0; H, 4.2; N, 6.5%).

$K[CrL_2]\cdot 2MeOH$. A solution of H_2L (0.070 g, 0.33 mmol), K_2CO_3 (0.022 g, 0.16 mmol) and [Cr(acac)$_3$] (Hacac = pentane-2,4-dione; 0.057 g, 0.16 mmol) in *n*-butanol (10 cm^3) was heated to 120 °C for 3 h, after which time a yellow precipitate had formed. After cooling the mixture this precipitate was filtered off, washed with Et_2O, and crystallised by diffusion of Et_2O vapour into a concentrated solution of the crude material in MeOH to give plate-like orange crystals (0.034 g, 40%). Negative-ion FAB mass spectrum: *m*/*z* 479 (100%, CrL_2) (Found: C, 52.9; H, 3.5; N, 5.0. $C_{26}H_{22}CrKN_2O_8$ requires C, 53.6; H, 3.8; N, 4.8%).

$K[FeL_2]\cdot 2MeOH$. To a slurry of H_2L (0.171 g, 0.8 mmol) and K_2CO_3 (0.055 g, 0.4 mmol) in water (30 cm^3) was added [Fe(acac)$_3$] (0.140 g, 0.4 mmol). The mixture was agitated in an ultrasound cleaning bath for 5 min and then stirred at room temperature for 2 d. The water was removed *in vacuo* and the residue crystallised by diffusion of Et_2O vapour into a concentrated solution of the crude material in MeOH to give red plate-like crystals (0.151 g, 65%). Negative-ion FAB mass spectrum: *m*/*z* 480 (100%, FeL_2) (Found: C, 52.7; H, 3.5; N, 5.3. $C_{26}H_{22}FeKN_2O_8$ requires C, 53.3; H, 3.8; N, 4.8%).

$[Cu_2L_2(MeOH)(H_2O)]$ and $[Cu_2L_2(MeOH)_2]$. A solution of H_2L (0.100 g, 0.47 mmol) in MeOH (20 cm^3) was added to a solution of copper(II) acetate hydrate (0.046 g, 0.23 mmol) in MeOH (20 cm^3), resulting in an immediate change to emerald green. The mixture was left to crystallise by slow evaporation. A crystalline mass formed which was filtered off and dried. Yield: 0.125 g, 98% (taking an average molecular weight for the two similar complexes). FAB mass spectrum: *m*/*z* 276 (100, CuL), 551 (30, $Cu_2L_2 - H$) and 704 (10%, Cu_2L_2 + matrix). Enough crystals of $[Cu_2L_2(MeOH)_2]$ could be separated manually for elemental analysis (Found: C, 50.8; H, 3.6; N, 4.7. $C_{26}H_{22}Cu_2N_2O_8$ requires C, 50.6; H, 3.6; N, 4.5%).

$K[ML_2(H_2O)]\cdot 2H_2O$ (M = Tb or Gd). A solution of H_2L (0.083 g, 0.39 mmol) and K_2CO_3 (0.107 g, 0.77 mmol) in water (20 cm^3) was added to a solution of the appropriate lanthanide chloride hydrate (0.20 mmol) in water (10 cm^3). A white precipitate formed which redissolved on stirring to give a yellow solution, which was left to crystallise by slow evaporation. The products were obtained in *ca*. 75% yield as clusters of small, colourless crystals. Crystallographic analysis (see Results and Discussion section) showed them both to be $K[ML_2(H_2O)_2]\cdot 2H_2O$ (M = Tb or Gd).

Data for $K[GdL_2(H_2O)_2]\cdot 2H_2O$: FAB mass spectrum (negative-ion mode) *m*/*z* 584 (80%, GdL_2) (Found: C, 41.2; H, 3.1; N, 4.0. $C_{24}H_{22}GdKN_2O_{10}$ requires C, 41.5; H, 3.2; N, 4.0%). Data for $K[TbL_2(H_2O)_2]\cdot 2H_2O$: FAB mass spectrum (negative-ion mode) *m*/*z* 585 (20%, TbL_2) and 214 (70%, HL). The elemental analyses for this complex varied considerably between runs, particularly in the %C values obtained; we have had this problem before with lanthanide complexes.[9]

X-Ray crystallography

Suitable crystals were quickly transferred from the mother-liquor to a stream of cold N_2 at −100 °C on a Siemens SMART diffractometer fitted with a CCD-type area detector. In all cases data were collected at −100 °C using graphite-monochromatised Mo-Kα radiation. A detailed experimental description of the methods used for data collection and integration using the SMART system has been published.[9] Table 1 contains a summary of the crystal parameters, and the data collection and refinement details. Empirical absorption corrections were applied to the datasets using SADABS.[15] The structures were solved by conventional heavy-atom or direct methods and refined by the full-matrix least-squares method on all F^2 data using the SHELXTL 5.03 package on a Silicon Graphics Indy computer.[16] Non-hydrogen atoms were refined with anisotropic thermal parameters; hydrogen atoms were included in calculated positions and refined with isotropic thermal parameters riding on those of the parent atom.

The structure determinations and refinements of $K[CrL_2]\cdot 2MeOH$, $K[FeL_2]\cdot 2MeOH$, $[Cu_2L_2(MeOH)(H_2O)]$ and $[Cu_2L_2(MeOH)_2]$ presented no unusual problems and were straightforward. Crystals of $K[TbL_2(H_2O)_2]\cdot 2H_2O$ were small intergrown plates and it proved difficult to isolate a fragment that was completely single. The best crystal that we could find (after several attempts) was not completely clear but had internal cracks and diffracted very weakly, displaying broad peak profiles. Although the structure of the complex is perfectly clear, the rather poor data quality has resulted in larger than normal residual electron-density peaks (+4.587 and −3.074 e $Å^{-3}$). These are not adjacent to the heavy metal and so do not correspond to absorption effects; nor are they in chemically reasonable positions for missing atoms (*e.g.* oxygen atoms of water molecules). Rather, they probably arise from the fact that the crystal was cracked and therefore possibly not single. The gadolinium(III) complex was also crystallographically studied, but the problems with crystal quality were worse and the result is therefore not included here, except to note that it is isomorphous and isostructural with the terbium(III) complex.

CCDC reference number 186/903.

Results and Discussion

Ligand synthesis

The synthesis of H_2L is outlined in Scheme 1. The starting material 2-(2-methoxyphenyl)pyridine is available in high yield from the heterocoupling of 2-bromopyridine and the Grignard

Table 1 Crystallographic data for the new complexes

Compound	$K[CrL_2]\cdot 2MeOH$	$K[FeL_2]\cdot 2MeOH$	$[Cu_2L_2(MeOH)(H_2O)]$	$[Cu_2L_2(MeOH)_2]$	$K[TbL_2(H_2O)_2]\cdot 2H_2O$
Formula	$C_{26}H_{22}CrKN_2O_8$	$C_{26}H_{22}FeKN_2O_8$	$C_{25}H_{20}Cu_2N_2O_8$	$C_{26}H_{22}Cu_2N_2O_8$	$C_{24}H_{22}KN_2O_{10}Tb$
M	581.56	585.41	603.51	617.54	696.46
System, space group	Triclinic, $P\bar{1}$	Triclinic, $P\bar{1}$	Monoclinic, $P2_1/c$	Monoclinic, $P2_1/c$	Monoclinic, $C2/c$
a/Å	8.033(2)	8.019(2)	15.425(3)	8.0366(9)	33.383(6)
b/Å	11.896(4)	12.025(3)	10.567(3)	9.9600(14)	10.080(3)
c/Å	13.084(3)	13.069(6)	14.225(4)	15.298(3)	14.983(3)
α/°	81.713(13)	80.53(3)			
β/°	75.610(13)	75.77(2)	100.76(2)	101.10(2)	94.250(13)
γ/°	87.86(2)	87.89(3)			
U/Å^3	1198.5(6)	1204.9(7)	2278.0(10)	1201.6(3)	5028(2)
Z	2	2	4	2	8
D_c/g cm^{-3}	1.612	1.614	1.760	1.707	1.840
μ/mm^{-1}	0.708	0.855	1.924	1.826	3.040
F(000)	598	602	1224	628	2752
Crystal size/mm	0.3 × 0.3 × 0.02	0.2 × 0.2 × 0.05	0.4 × 0.4 × 0.2	0.5 × 0.2 × 0.2	0.3 × 0.3 × 0.05
Reflections collected: total, independent R_{int}	12 441, 5429, 0.0358	10 448, 4241, 0.0440	18 519, 408, 0.1028	7431, 2737, 0.0264	16 354, 3282, 0.0732
2θ Limits for data/°	3–55	3–50	5–50	5–55	3–45
Data, restraints, parameters	5429, 0, 353	4240, 0, 347	4005, 0, 335	2737, 0, 177	3280, 36, 343
Final $R1$, $wR2$[a,b]	0.0382, 0.0993	0.0427, 0.1058	0.0584, 0.1548	0.0261, 0.0667	0.0808, 0.2399
Weighting factors[b]	0.0482, 0.0769	0.0555, 0	0.0826, 0	0.0352, 0	0.1780, 0
Largest peak, hole/e Å^{-3}	+0.321, −0.516	+0.629, −0.644	+1.415, −1.034	+0.305, −0.488	+4.587, −3.074

[a] Structure was refined on F_o^2 using all data; the value of $R1$ is given for comparison with older refinements based on F_o with a typical threshold of $F \geqslant 4\sigma(F)$. [b] $wR_2 = \{\Sigma[w(F_o^2 - F_c^2)^2]/\Sigma w(F_o^2)^2\}^{\frac{1}{2}}$ where $w^{-1} = [\sigma^2(F_o^2) + (aP)^2 + bP]$ and $P = [\max(F_o^2, 0) + 2F_c^2]/3$.

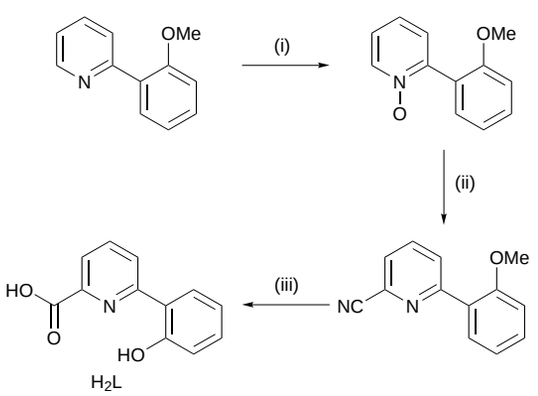

Scheme 1 (i) H_2O_2, glacial acetic acid; (ii) Me_3SiCN, Et_3N, MeCN; (iii) HI

reagent of 2-bromoanisole, catalysed by $[Ne(dppe)Cl_2]$.[11] Conversion of this into the *N*-oxide followed by reaction with Me_3SiCN adds a cyano group to the pyridyl nucleus, to give 2-cyano-6-(2-hydroxyphenyl)pyridine. The final step is acid hydrolysis, which conveniently performs two functions: it demethylates the anisole to liberate the phenol, and simultaneously hydrolyses the cyano group to a carboxylic acid to give H_2L. All of the steps work well with high yields. The compound H_2L was characterised satisfactorily from its elemental analysis, and its mass and ^{1}H NMR spectra; in particular the phenolic OH proton resonates at δ *ca.* 14 due to formation of an intramolecular hydrogen bond with the pyridyl N atom.[11,17]

Complexes with Cr^{III} and Fe^{III}

Reaction of H_2L and base (potassium carbonate) with $[M(acac)_3]$ (M = Cr or Fe) afforded, by ligand exchange, complexes of L. The more vigorous conditions required to prepare the chromium(III) complex reflects its greater kinetic inertness. Negative-ion FAB mass spectra gave a strong signal for $[ML_2]^-$ in each case, confirming formation of mononuclear (presumably six-co-ordinate) complexes in which the ligands are doubly deprotonated. Elemental analyses indicated that the cation was K^+.

X-Ray-quality crystals of both complexes were isolated from MeOH–diethyl ether; the structures are very similar (Fig. 1 and 2; Table 2). Both complexes have the formulation $K[ML_2]\cdot 2MeOH$. In both cases the metal ions are in approximately octahedral geometries from two meridionally co-ordinated ligands, resulting in a *cis*,*trans*,*cis*–$O_2N_2O'_2$ co-ordination geometry, and one six- and one five-membered chelate ring associated with each ligand (Fig. 1). The ligands are not planar due to a twist between the aromatic pyridyl and phenolate rings.

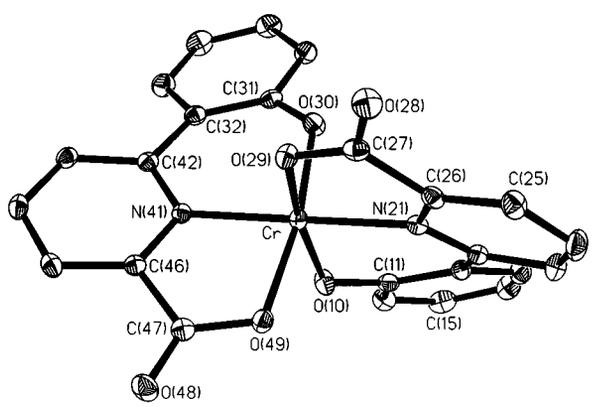

Fig. 1 Crystal structure of the complex anion of $K[CrL_2]\cdot 2MeOH$

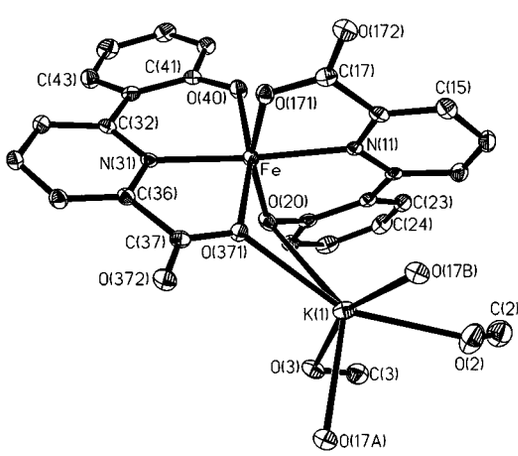

Fig. 2 Crystal structure of $K[FeL_2]\cdot 2MeOH$

Table 2 Selected bond lengths (Å) and angles (°) for K[ML_2]·2MeOH (M = Cr or Fe)

Cr–O(30)	1.905(2)	Fe–O(20)	1.904(2)
Cr–O(10)	1.908(2)	Fe–O(40)	1.905(2)
Cr–O(49)	1.997(2)	Fe–O(371)	2.030(2)
Cr–O(29)	2.009(2)	Fe–O(171)	2.041(2)
Cr–N(41)	2.021(2)	Fe–N(31)	2.120(3)
Cr–N(21)	2.038(2)	Fe–N(11)	2.159(3)
K(2)–O(1)	2.673(2)	K(1)–O(3B)	2.696(3)
K(2)–O(3)	2.706(2)	K(1)–O(172)	2.731(3)
K(2)–O(49)	2.723(2)	K(1)–O(2B)	2.744(3)
K(2)–O(28A)	2.746(2)	K(1)–O(371A)	2.768(2)
K(2)–O(28B)	2.781(2)	K(1)–O(172B)	2.771(3)
K(2)–O(10)	3.298(2)	K(1)–O(20A)	3.064(3)
O(30)–Cr–O(10)	96.26(8)	O(20)–Fe–O(40)	100.86(10)
O(30)–Cr–O(49)	171.21(7)	O(20)–Fe–O(371)	86.27(10)
O(10)–Cr–O(49)	87.94(8)	O(40)–Fe–O(371)	164.47(9)
O(30)–Cr–O(29)	89.65(8)	O(20)–Fe–O(171)	158.99(10)
O(10)–Cr–O(29)	168.49(7)	O(40)–Fe–O(171)	90.62(10)
O(49)–Cr–O(29)	87.60(7)	O(371)–Fe–O(171)	87.12(9)
O(30)–Cr–N(41)	90.58(8)	O(20)–Fe–N(31)	103.95(10)
O(10)–Cr–N(41)	97.08(8)	O(40)–Fe–N(31)	86.46(10)
O(49)–Cr–N(41)	81.22(7)	O(371)–Fe–N(31)	78.39(10)
O(29)–Cr–N(41)	92.71(7)	O(171)–Fe–N(31)	94.19(10)
O(30)–Cr–N(21)	92.61(8)	O(20)–Fe–N(11)	84.17(10)
O(10)–Cr–N(21)	88.89(8)	O(40)–Fe–N(11)	94.78(10)
O(49)–Cr–N(21)	95.19(7)	O(371)–Fe–N(11)	99.69(10)
O(29)–Cr–N(21)	80.97(7)	O(171)–Fe–N(11)	77.33(10)
N(41)–Cr–N(21)	172.89(8)	N(31)–Fe–N(11)	171.43(10)

In the chromium(III) structure the dihedral angles between mean planes of aromatic rings are 20.0 and 23.4° between rings 1/2 and 3/4 respectively [where ring 1 is C(11)–C(16), *etc.*]; in the iron(III) structure the values are 24.9 and 20.7° between rings 1/2 and 3/4 respectively. The metal–ligand bond lengths are typical for chromium(III) and high-spin iron(III) complexes. Low-spin Fe^{III} is relatively rare and has significantly shorter metal–ligand bond distances than high-spin Fe^{III}, and the high-spin nature of $[FeL_2]^-$ was also confirmed spectroscopically (below).

The anionic complex units are held together in the crystals by cross-linking with a K^+ cation. Each K^+ ion forms two interactions to an adjacent complex unit, involving one phenolate and one carboxylate oxygen atom; these oxygen atoms are therefore bridging between the transition metal ion and the K^+ ion. The K^+ ion is also co-ordinated by an externally directed carboxylate oxygen atom (*i.e.* the one that is not co-ordinated to the transition-metal centre) from two different complex units, as well as two methanol molecules, making it six-co-ordinate overall and interacting with three different complex units.

The electronic spectrum of K[CrL_2] in solution is consistent with the geometry seen in the crystal structures. For octahedral chromium(III) complexes three d–d transitions are expected, of which the lowest-energy transition $^4A_{2g}(F) \longrightarrow {}^4T_{2g}(F)$, corresponding to Δ_{oct}, is visible at 556 nm (17 900 cm^{-1}) with an absorption coefficient (ε) of *ca.* 100 $dm^3\ mol^{-1}\ cm^{-1}$. The ligand-field strength is therefore similar to those of complexes with O-donor ligand sets such as $[Cr(H_2O)_6]^{3+}$ (17 400 cm^{-1}) and $[Cr(C_2O_4)_3]^{3-}$ (17 500 cm^{-1}), and considerably weaker than in complexes with N-donor ligand sets. The two higher-energy d–d transitions are obscured by the much more intense transitions in the UV region. Of these, the weaker transition, a shoulder at 370 nm (ε *ca.* 2000 $dm^3\ mol^{-1}\ cm^{-1}$), could be a phenolate[$O(p_\pi)$]→$Cr(d_\pi)$ ligand-to-metal charge-transfer (LMCT), by analogy with the iron(III) complex (below). The two very intense transitions at 328 and 267 nm are ligand-centred π–π* transitions.

For high-spin Fe^{III} no d–d transitions are expected and all of the transitions are therefore ligand-to-metal charge transfer, or ligand-centred, in origin. The most significant feature of the spectrum is the phenolate[$O(p_\pi)$] ⟶ $Fe(d_\pi)$ LMCT band at

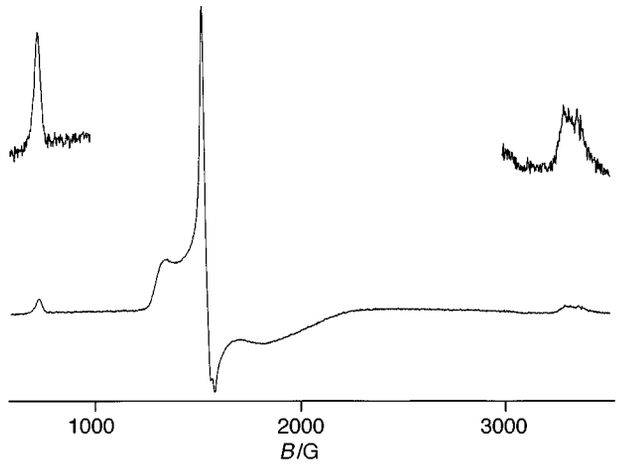

Fig. 3 X-Band EPR spectrum of K[FeL_2] in a MeOH–thf glass at 77 K

490 nm (ε 1400 $dm^3\ mol^{-1}\ cm^{-1}$).[4,18] This is a very characteristic feature of iron(III)–phenolate complexes, including the iron(III)–tyrosinate proteins, and both the energy and intensity of this transition are in good agreement with those of both the natural systems[2,3] and their synthetic analogues.[4] The UV transitions are again predominantly ligand-centred π–π* transitions.

The EPR spectrum of K[FeL_2] (Fig. 3) also confirms that the complex is high spin, and is characteristic of a pseudo-octahedral ligand field with rhombic distortion.[19] In perfect rhombic symmetry an isotropic signal at $g \approx 4.3$ is expected from the middle Kramers doublet. The transitions within the upper and lower Kramers doublets behave similarly to each other, both giving a very anisotropic signal with one component at $g \approx 9$, and the other two components at $g \approx 0.7$ which are generally not observed. The spectrum of K[FeL_2] conforms approximately to this, but with some obvious perturbations. Most importantly the main signal from the middle Kramers doublet is not isotropic, but clearly has three components at g values of 5.00 (upward-pointing), 4.35 (sharp inflexion) and 3.70 (downward-pointing). The characteristic low-field signal is at $g = 9.17$. Also present is a weak signal at $g = 2.03$ which is not expected for an ideal rhombic system, but which probably arises because the ligand-field symmetry is distorted from ideal rhombic symmetry (as shown by the anisotropy of the $g \approx 4.3$ signal). A tetragonal component to the geometry, for example, would result in a $g \approx 2$ transition.[19] Low-spin Fe^{III} also has a signal at $g \approx 2$ but this possibility clearly cannot apply here.

Electrochemical studies on the complexes in dmf revealed little of interest beyond ill defined, irreversible processes at high positive and negative potentials. It has been noted for a related iron(III) complex that a reversible Fe^{III}–Fe^{II} couple can be seen by cyclic voltammetry in water but not in dmf,[4] but our complexes were not sufficiently water-soluble to check this.

Complexes with Cu^{II}

Reaction of H_2L with copper(II) acetate in MeOH afforded a neutral complex which, according to elemental analysis, had a 1:1 metal:ligand ratio. Crystallisation by slow evaporation from MeOH afforded two visibly different types of crystal which were intergrown, but X-ray-quality fragments of each type could be separated by hand. The structures are in Figs. 4 and 5, and reveal that the two complexes have the same dinuclear core structure and differ only in the nature of the co-ordinated solvent molecules.

In both [$Cu_2L_2(MeOH)(H_2O)$] (Fig. 4, Table 3) and [$Cu_2L_2(MeOH)_2$] (Fig. 5, Table 4) there is a roughly planar Cu_2L_2 unit, with a $Cu_2(\mu\text{-}O)_2$ core arising from two bridging phenolate groups. This results in an approximately square-planar O_3N co-ordination environment around each metal with metal–ligand

Table 3 Selected bond lengths (Å) and angles (°) for $[Cu_2L_2(MeOH)(H_2O)]$

Cu(1)–N(11)	1.935(5)	Cu(2)–O(40)	1.908(4)
Cu(1)–O(20)	1.939(4)	Cu(2)–O(39)	1.919(4)
Cu(1)–O(40)	1.954(4)	Cu(2)–N(31)	1.959(5)
Cu(1)–O(19)	1.959(4)	Cu(2)–O(20)	2.003(4)
Cu(1)–O(6)	2.239(4)	Cu(2)–O(5)	2.319(4)
Cu(1)···Cu(2)	3.0113(12)		
N(11)–Cu(1)–O(20)	93.1(2)	O(40)–Cu(2)–O(39)	168.1(2)
N(11)–Cu(1)–O(40)	169.2(2)	O(40)–Cu(2)–N(31)	91.7(2)
O(20)–Cu(I)–O(40)	79.0(2)	O(39)–Cu(2)–N(31)	84.8(2)
N(11)–Cu(1)–O(19)	84.3(2)	O(40)–Cu(2)–O(20)	78.5(2)
O(20)–Cu(1)–O(19)	160.3(2)	O(39)–Cu(2)–O(20)	101.4(2)
O(40)–Cu(1)–O(19)	100.6(2)	N(31)–Cu(2)–O(20)	160.5(2)
N(11)–Cu(1)–O(6)	93.5(2)	O(40)–Cu(2)–O(5)	96.3(2)
O(20)–Cu(1)–O(6)	104.8(2)	O(39)–Cu(2)–O(5)	95.6(2)
O(40)–Cu(1)–O(6)	95.7(2)	N(31)–Cu(2)–O(5)	104.3(2)
O(19)–Cu(1)–O(6)	94.8(2)	O(20)–Cu(2)–O(5)	93.6(2)

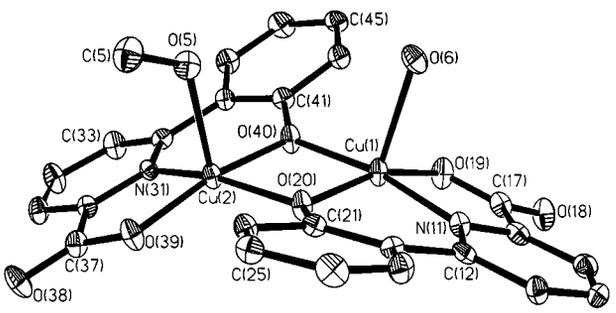

Fig. 4 Crystal structure of $[Cu_2L_2(MeOH)(H_2O)]$

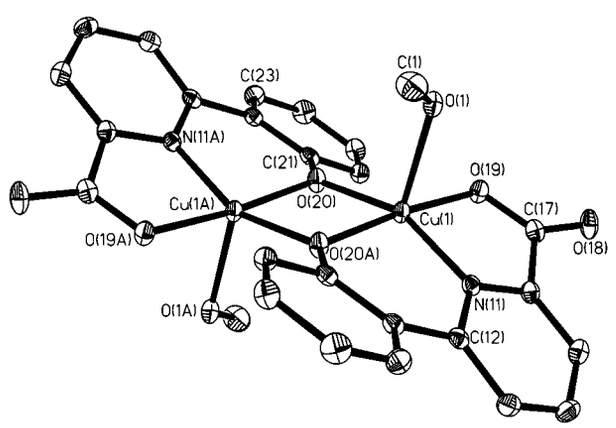

Fig. 5 Crystal structure of $[Cu_2L_2(MeOH)_2]$

bond lengths in the range 1.9–2.0 Å. In both complexes a fifth O-donor ligand (a co-ordinated solvent molecule) is also present at each metal site, with a Cu–O separation in the range 2.24–2.32 Å, resulting in the elongated square-pyramidal geometry that is characteristic of Cu^{II} because of the Jahn–Teller effect. In $[Cu_2L_2(MeOH)(H_2O)]$ the axial ligands are H_2O at Cu(1) and MeOH at Cu(2). Both of these lie on the same face of the Cu_2L_2 core. In $[Cu_2L_2(MeOH)_2]$ however both Cu atoms have a methanol molecule as the fifth axial ligand, and these point in opposite directions such that there is one on each face of the Cu_2L_2 core. This results in $[Cu_2L_2(MeOH)_2]$ having an additional symmetry element (an inversion centre) which is not present in $[Cu_2L_2(MeOH)(H_2O)]$, making both metal ions crystallographically equivalent. The Cu···Cu separations are 3.01 and 3.02 Å in $[Cu_2L_2(MeOH)(H_2O)]$ and $[Cu_2L_2(MeOH)_2]$ respectively.

An additional consequence of the differing disposition of co-ordinated solvent molecules is that the distortions of the Cu_2L_2 cores from planarity are quite different in the two complexes. In

Table 4 Selected bond lengths (Å) and angles (°) for $[Cu_2L_2(MeOH)_2]$

Cu(1)–O(20A)	1.9254(13)	Cu(1)–O(20)	1.9774(13)
Cu(1)–O(19)	1.9376(13)	Cu(1)–O(1)	2.256(2)
Cu(1)–N(11)	1.955(2)	Cu(1)···Cu(1A)	3.0203(6)
O(20A)–Cu(1)–O(19)	173.89(6)	N(11)–Cu(1)–O(20)	156.01(7)
O(20A)–Cu(1)–N(11)	91.97(6)	O(20A)–Cu(1)–O(1)	98.64(6)
O(19)–Cu(1)–N(11)	84.60(6)	O(19)–Cu(1)–O(1)	87.03(6)
O(20A)–Cu(1)–O(20)	78.60(6)	N(11)–Cu(1)–O(1)	101.77(6)
O(19)–Cu(1)–O(20)	102.61(6)	O(20)–Cu(1)–O(1)	101.44(6)

$[Cu_2L_2(MeOH)(H_2O)]$ (Fig. 4) there is an overall curvature of the Cu_2L_2 core, which helps to remove any unfavourable steric interactions between the axial solvent ligands. In consequence the two metal co-ordination planes (defined as the mean plane through the four basal donor atoms) are at an angle of 25.1° to one another, which may be envisaged as a fold about the O(20)···O(40) vector. For the two planes thus defined, all four atoms involved deviate from the mean plane through them by less than 0.1 Å [plane around Cu(1)] or 0.06 Å [plane around Cu(2)]. The metal atoms are displaced out of their mean co-ordination planes towards the axial ligand by 0.240 Å [Cu(1)] and 0.251 Å [Cu(2)]. The torsion angles between the mean planes of the two aromatic rings of each ligand are 12.1 (between rings 1 and 2) and 10.9° (between rings 3 and 4).

For $[Cu_2L_2(MeOH)_2]$ (Fig. 5) in contrast the inversion centre means that there can be no curvature of the Cu_2L_2 core, and indeed the transoid arrangement of the axial ligands means that this curvature is no longer necessary to alleviate steric interactions between them. Consequently the two metal co-ordination planes (again defined as the mean plane of the four donor atoms in the basal plane) are parallel and coplanar. The four basal donor atoms [N(11), O(19), O(20), O(20A)] do not make quite such good planes as were found in $[Cu_2L_2(MeOH)(H_2O)]$, with deviations of up to 0.14 Å from the mean plane through them. The metal atom is displaced by 0.239 Å out of this plane towards the axial methanol ligand.

For solution spectroscopic studies we made no attempt to separate the different types of crystalline material, as we thought it safe to assume that rapid exchange of the labile axial ligands would render the two species equivalent. Apart from the usual intense bands in the UV region of the electronic spectrum, a d–d transition is also apparent at 664 nm (ε *ca.* 300 dm^3 mol^{-1} cm^{-1}), which is consistent with the expected tetragonal co-ordination geometry. The solution EPR spectra were slightly surprising, giving at 77 K in a MeOH–thf glass a typical *mononuclear* copper(II) spectrum with $g_{\|} = 2.28$, $g_{\perp} = 2.06$, $A_{\|} = 166$ G. There is no sign of any of the characteristic features of a triplet spectrum,[20] indicating that in the polar solvents in which the complexes dissolve (dmf, MeOH) cleavage of the $Cu_2(\mu\text{-}O)_2$ bridge, which is unsupported by any additional bridging ligands, occurs. A room-temperature powder spectrum of $[Cu_2L_2(MeOH)(H_2O)]$ however, although broad and poorly defined, showed a half-field signal at 1723 G ($g = 4.04$) corresponding to the $\Delta m_s = 2$ transition to be expected for the intact dinuclear species, in addition to the principal $\Delta m_s = 1$ transition at 3310 G ($g = 2.11$).

Magnetic susceptibility measurements on a powdered microcrystalline sample showed that the two copper(II) ions are strongly antiferromagnetically coupled, with the magnetic moment μ per copper(II) decreasing from 1.50 μ_B at room temperature to 0.64 μ_B at 78 K. The data however did not fit the Bleaney–Bowers equation well, probably because the microcrystalline sample is a mixture of $[Cu_2L_2(MeOH)(H_2O)]$ and $[Cu_2L_2(MeOH)_2]$ (*cf.* Figs. 4 and 5), in which the relative orientations of the magnetic orbitals [$d(x^2 - y^2)$, the basal plane of the square pyramid] are appreciably different. It is also possible, given the complete dissociation of the dimer into monomeric units in solution, that a trace of a mononuclear species in the

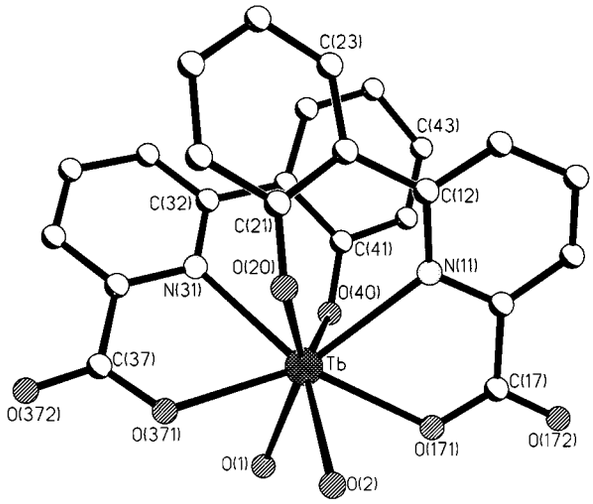

Fig. 6 Crystal structure of $K[TbL_2(H_2O)_2]\cdot 2H_2O$

solid state will further complicate matters. We therefore have not analysed the magnetic data further, but we note that strong antiferromagnetic exchange (typically a few hundred cm^{-1}) is to be expected from the side-by-side arrangement of $d(x^2 - y^2)$ orbitals which allows effective overlap between them,[21] in contrast to the weaker interaction which occurs over similar Cu···Cu separations when the magnetic orbitals are 'face-to-face' and therefore do not overlap so well.[20]

Complexes with lanthanide(III) ions

Reaction of H_2L with lanthanide(III) salts (Tb, Gd) in aqueous solution resulted in the slow formation of a crystalline material in each case. In the negative-ion FAB mass spectra the principal peak in each case corresponded to the species $[ML_2]^-$, and the elemental analysis of the gadolinium complex was consistent with the formulation $K[GdL_2]\cdot 4H_2O$, which was subsequently confirmed crystallographically. We found no evidence for formation of $[ML_3]^{3-}$ species, in contrast to the well established formation of 3:1 ligand:metal complexes between pyridine-2,6-dicarboxylate (like L^{2-}, a terdentate, dianionic O,N,O-donor ligand) and lanthanides.[22]

The crystal structure of $K[TbL_2(H_2O)_2]\cdot 2H_2O$ (Fig. 6, Table 5) shows the terbium(III) centre to be eight-co-ordinate, from two terdentate ligands L^{2-} and two co-ordinated water molecules. The co-ordination geometry is very approximately square antiprismatic, with atoms N(31), O(371), O(40), O(1) describing one approximate plane and O(2), N(11), O(171), O(20) the other, and an angle of intersection of 6° between these two mean planes. There is a some overlap between sections of the two independent aromatic ligands, leading to a π-stacking interaction.

The complex anions are held together by an extensive network of ionic bonds involving the K^+ ions, and also by intramolecular hydrogen bonds involving water ligands. Each K^+ ion interacts with water [O(2)] and phenolate [O(20)] oxygen donors of one complex unit; with the externally directed, non-co-ordinated oxygen atoms [O(172) and O(372)] from two further adjacent complex units, and a water oxygen atom [O(2)] from a fourth complex unit. Each K^+ ion has in addition two terminal water ligands [O(3) and O(4)] and is therefore seven-co-ordinate overall with K–O separations in the range 2.68–3.18 Å. Intracomplex hydrogen-bonding interactions occur between the water ligand O(3) attached to a K^+ ion and O(40) of another complex anion (non-bonded O···O separation, 2.76 Å), and between the water ligand O(1) of one complex unit and the carboxylate atom O(172) of another (non-bonded O···O separation, 2.76 Å).

The crystal structure of the gadolinium(III) analogue $K[GdL_2(H_2O)_2]\cdot 2H_2O$ was also determined, but is not described in any detail because splitting of the peak profiles in all of the crystals that we tried meant that the level of refinement is poor. However it was clear that this complex is isostructural and isomorphous with the terbium(III) complex.

Table 5 Selected bond lengths (Å) and angles (°) for $K[TbL_2(H_2O)_2]\cdot 2H_2O$

Tb–O(40)	2.280(9)	Tb–O(1)	2.433(10)
Tb–O(20)	2.310(10)	Tb–O(2)	2.442(10)
Tb–O(171)	2.393(9)	Tb–N(31)	2.554(12)
Tb–O(371)	2.398(10)	Tb–N(11)	2.558(10)
O(40)–Tb–O(20)	124.8(3)	O(1)–Tb–O(2)	87.8(4)
O(40)–Tb–O(171)	79.3(3)	O(40)–Tb–N(31)	68.6(4)
O(20)–Tb–O(171)	120.1(3)	O(20)–Tb–N(31)	78.5(4)
O(40)–Tb–O(371)	122.7(4)	O(171)–Tb–N(31)	147.8(4)
O(20)–Tb–O(371)	78.6(4)	O(371)–Tb–N(31)	67.2(4)
O(171)–Tb–O(371)	138.1(3)	O(1)–Tb–N(31)	94.8(4)
O(40)–Tb–O(1)	76.2(3)	O(2)–Tb–N(31)	141.1(4)
O(20)–Tb–O(1)	151.5(3)	O(40)–Tb–N(11)	76.7(3)
O(171)–Tb–O(1)	79.7(3)	O(20)–Tb–N(11)	69.0(3)
O(371)–Tb–O(1)	73.3(4)	O(171)–Tb–N(11)	65.7(3)
O(40)–Tb–O(2)	148.3(3)	O(371)–Tb–N(11)	147.5(4)
O(20)–Tb–O(2)	80.9(4)	O(1)–Tb–N(11)	139.2(3)
O(171)–Tb–O(2)	70.8(3)	O(2)–Tb–N(11)	99.9(3)
O(371)–Tb–O(2)	76.7(4)	N(31)–Tb–N(11)	102.9(4)

Information on the solvation state of luminescent lanthanide complexes may be obtained by comparison of the luminescence lifetimes in protonated and deuteriated solvents (water and methanol) using the Horrocks equation, which gives an approximate value for the number of co-ordinated solvent molecules in solution.[23,24] Excitation of a MeOH solution of $K[TbL_2(H_2O)_2]\cdot 2H_2O$ at 266 nm (into one of the ligand-centred π–π* transitions) shows the expected sequence of $^5D_4 \longrightarrow {}^7F_n$ transitions, with the $n = 6$, 5, 4 and 3 components being visible; no further splitting of these was visible and the spectrum is entirely typical.[9] Time-resolved measurement of the emission intensity at 546 nm, the emission maximum, following excitation with a 10 μs pulse, resulted in a single exponential decay with a lifetime τ_H of 0.81 ms. In CD_3OD however the emission lifetime τ_D was 1.61 ms. Using equation (1) gives q (the number

$$q = 8.4\,(\tau_H^{-1} - \tau_D^{-1}) \qquad (1)$$

of co-ordinated solvent molecules in methanol solution) as 4.9, with an error of ±0.5.[22] Attempts to measure lifetimes in H_2O/D_2O were unsuccessful as the luminescence intensity dropped to nearly zero, consistent with a substantial degree of ligand dissociation induced by the competing solvent donors.

If both ligands L^{2-} remained fully co-ordinated in MeOH solution we might expect an additional two or three solvent molecules to co-ordinate directly, giving a total of eight- or nine-co-ordination which is normal for Tb^{3+}. Thus the value of 4.9 for q seems high even allowing for the usually quoted error of ±0.5. There are two possible reasons for this. First, Parker and co-workers[23,24] have shown for a series of luminescent complexes of Tb and Eu that solvent molecules in a secondary co-ordination sphere, particularly those associated by hydrogen bonding, can also make a contribution to the value of q whose magnitude depends on their proximity to the metal centre. However the effect is considerably larger for complexes of Eu than for those of Tb where this contribution to q was in the range $0 < q < 0.4$.[24] The anion $[TbL_2(H_2O)_2]^-$ is clearly capable of hydrogen bonding to methanol molecules in solution *via* the pendant non-co-ordinated carboxylate oxygen atoms (*cf.* the crystal structure), so there will be a contribution to q, albeit rather small, from this effect.

The second, and probably more substantial, contribution to the high value of q is likely to be partial dissociation of the terdentate ligands. Such behaviour has been established for

example in $[Eu(terpy)_3]^{3+}$, which in MeCN solution can undergo a ligand-based conformational rearrangement involving rotation of terminal pyridyl rings about the interannular C–C bonds, resulting in dissociation of the terminal pyridyl rings and solvent co-ordination.[25] We attempted to check this by seeing if the electronic spectra of the complex in MeOH solution showed any clear evidence for dissociation. The electronic spectrum of $K[TbL_2(H_2O)_2]$ showed UV transitions at 333 and 265 nm in neat MeOH, which are slightly blue-shifted to 325 and 262 nm in MeOH–water (2:1), consistent with some degree of dissociation of the aromatic ligands from the positively charged metal centre in the presence of water. We know from the near absence of an emission spectrum that water induces substantial ligand dissociation, and in fact the electronic spectrum of $K[TbL_2(H_2O)_2]$ in the presence of water is very similar to that of free L^{2-} (in aqueous KOH), in which the UV transitions are at 325 and 260 nm. The implication of this is that MeOH alone is not a good enough ligand to induce complete ligand dissociation, although *partial* dissociation, *e.g.* just of the terminal phenolate rings to give bidentate co-ordination of one or both L^{2-} ligands, is quite possible and cannot be ruled out on this evidence.

Acknowledgements

We thank the EPSRC for a studentship (to S. M. C.), and Dr. John Maher for assistance with the EPR spectroscopy.

References

1 D. A. Bardwell, D. Black, J. C. Jeffery, E. Schatz and M. D. Ward, *J. Chem. Soc.*, *Dalton Trans.*, 1993, 2321; D. A. Bardwell, J. C. Jeffery, E. Schatz, E. E. M. Tilley and M. D. Ward, *J. Chem. Soc.*, *Dalton Trans.*, 1995, 825; D. A. Bardwell, J. C. Jeffery and M. D. Ward, *J. Chem. Soc.*, *Dalton Trans.*, 1995, 3071; A. M. W. Cargill Thompson, D. A. Bardwell, J. C. Jeffery, L. H. Rees and M. D. Ward, *J. Chem. Soc.*, *Dalton Trans.*, 1997, 721; A. M. W. Cargill Thompson, S. R. Batten, J. C. Jeffery, L. H. Rees and M. D. Ward, *Aust. J. Chem.*, 1997, **50**, 109.
2 L. Que, jun. and A. E. True, *Prog. Inorg. Chem.*, 1990, **38**, 97.
3 L. Que, jun., *Coord. Chem. Rev.*, 1983, **50**, 73.
4 M. R. McDevitt, A. W. Addison, E. Sinn and L. K. Thompson, *Inorg. Chem.*, 1990, **29**, 3425.
5 L. Casella, M. Gullotti, A. Pintar, L. Messori, A. Rockenbauer and M. Györ, *Inorg. Chem.*, 1987, **26**, 1031.
6 H. U. Naegeli and H. Zähnder, *Helv. Chim. Acta*, 1980, **63**, 1400; F. E. Hahn, T. J. McMurry, A. Hugi and K. N. Raymond, *J. Am. Chem. Soc.*, 1990, **112**, 1854.
7 K. Langemann, D. Heineke, S. Rupprecht and K. N. Raymond, *Inorg. Chem.*, 1996, **35**, 5663.
8 A. P. de Silva, H. Q. N. Gunaratne and T. E. Rice, *Angew. Chem.*, *Int. Ed. Engl.*, 1996, **35**, 2116; P. A. Brayshaw, J.-C. G. Bünzli, P. Froidevaux, J. M. Harrowfield, Y. Kim and A. N. Sobolev, *Inorg. Chem.*, 1995, **34**, 2068; J. B. Lamture, Z. H. Zhou, A. S. Kumar and T. G. Wensel, *Inorg. Chem.*, 1995, **34**, 864; M. Latva, H. Takalo, K. Simberg and J. Kankare, *J. Chem. Soc.*, *Perkin Trans. 2*, 1995, 995.
9 P. L. Jones, A. J. Amoroso, J. C. Jeffery, J. A. McCleverty, E. Psillakis, L. H. Rees and M. D. Ward, *Inorg. Chem.*, 1997, **36**, 10.
10 D. A. Bardwell, J. C. Jeffery, P. L. Jones, J. A. McCleverty, E. Psillakis, Z. Reeves and M. D. Ward, *J. Chem. Soc.*, *Dalton Trans.*, 1997, 2079; N. Armaroli, V. Balzani, F. Barigelletti, M. D. Ward and J. A. McCleverty, *Chem. Phys. Lett.*, 1997, **276**, 435.
11 B. M. Holligan, J. C. Jeffery, M. K. Norgett, E. Schatz and M. D. Ward, *J. Chem. Soc.*, *Dalton Trans.*, 1992, 3345.
12 M. A. Laffey and P. Thornton, *J. Chem. Soc.*, *Dalton Trans.*, 1982, 313.
13 E. J. Corey, A. L. Borror and T. Foglia, *J. Org. Chem.*, 1965, **30**, 288.
14 T. Sakamoto, S. Kaneda, S. Nishimura and H. Yamanaka, *Chem. Pharm. Bull.*, 1985, **33**, 565; H. Vorbruggen and K. Krolikiewicz, *Synthesis*, 1983, 316.
15 SADABS, G. M. Sheldrick, University of Göttingen, 1996.
16 SHELXTL 5.03 program system, Siemens Analytical X-Ray Instruments, Madison, WI, 1995.
17 J. C. Jeffery, C. S. G. Moore, E. Psillakis, M. D. Ward and P. Thornton, *Polyhedron*, 1995, **14**, 509.
18 B. P. Gaber, V. Miskowski and T. G. Spiro, *J. Am. Chem. Soc.*, 1974, **96**, 6868.
19 W. T. Oosterhuis, *Struct. Bonding* (*Berlin*), 1974, **20**, 59.
20 J. P. Maher, P. H. Rieger, P. Thornton and M. D. Ward, *J. Chem. Soc.*, *Dalton Trans.*, 1992, 3353.
21 O. Kahn, *Angew. Chem.*, *Int. Ed. Engl.*, 1985, **24**, 834; M. Kato and Y. Muto, *Coord. Chem. Rev.*, 1988, **92**, 45.
22 W. D. Horrocks and D. R. Sudnick, *Acc. Chem. Res.*, 1981, **14**, 384; N. Sabbatini, M. Guardigli and J.-M. Lehn, *Coord. Chem. Rev.*, 1993, **123**, 201.
23 D. Parker and J. A. G. Williams, *J. Chem. Soc.*, *Dalton Trans.*, 1996, 3613.
24 S. Aime, M. Botta, D. Parker and J. A. G. Williams, *J. Chem. Soc.*, *Dalton Trans.*, 1996, 17.
25 R. D. Chapman, R. T. Loda, R. W. Riehl and R. W. Schwartz, *Inorg. Chem.*, 1984, **23**, 1652.

Received 18*th December* 1997; *Paper* 7/09078A